International Journal of Thermophysics, Vol. 20, No. 1, 1999

System for Measuring the Spectral Distribution of Normal Emissivity of Metals with Direct Current Heating[1]

M. Kobayashi,[2,3] M. Otsuki,[2] H. Sakate,[2] F. Sakuma,[2] and A. Ono[2,3]

A system for measuring time variations of the normal spectral emissivity at wavelengths ranging from 0.55 to 5.3 μm was developed and applied to metal specimens in vacuum and oxidizing environments in the temperature range from 780 to 1200° C. The specimen was heated to high temperatures by passing a direct current in a vacuum chamber, and the surface oxidation was controlled by a low-pressure oxidizing gas. The specimen temperature was measured by a single-band (0.9-μm) radiation thermometer viewing at a cavity formed in the specimen from the rear side. The front surface of the specimen was observed by a multiband (112-wavelength) radiation thermometer to measure the normal spectral emissivity. The effective normal spectral emissivity of the specimen cavity was evaluated to be 0.94 ± 0.05 at a wavelength of 0.9 μm in comparison with a metal tube having a small blackbody hole on the rear. The measurement uncertainty of the normal spectral emissivitiy by the system was estimated to be 5 to 10% of the emissivity value in most of the interesting ranges of emissivities, temperatures, and wavelengths.

KEY WORDS: high temperature; metal; spectral emissivity; oxidation; radiation thermometer.

1. INTRODUCTION

A knowledge of the spectral emissivity of a target is essential for measurements of temperature by thermal radiation. However, the emissivity can easily change due to physical and chemical conditions of the surface,

[1] Paper presented at the Thirteenth Symposium on Thermophysical Properties, June 22–27, 1997, Boulder, Colorado, U.S.A.

[2] Thermophysical Metrology Department, National Research Laboratory of Metrology, 1-4, Umezono 1-chome, Tsukuba-shi, Ibaraki 305, Japan.

[3] To whom correspondence should be addressed.

0195-928X/99/0100-0289$16.00/0

especially to surface oxidation for metals. Changes in the spectral emissivity of metals have been investigated during oxidation processes at selected wavelengths [1–3], and oscillations of the spectral emissivity have been observed for some metals as surface oxidation progresses. It is understood from those investigations that accurate temperature measurements of metal surfaces need a new technique of radiation thermometry rather than conventional single-band or two-band radiation thermometers.

Recent developments in electronics have made it easier to realize high performance multiband radiation thermometers [4]. Spectral radiance measurements covering a wide wavelength range at continuous wavelengths for a short scanning period are now available through improvements of infrared array detectors and signal processors. New multiband radiation thermometers seem promising to have a possibility of emissivity compensation for radiation thermometry of metals in oxidation processes.

Makino [5] has developed a high-speed spectrometer, and measured time variations of the spectral reflectivity of metals in an oxidizing environment at high temperatures [6]. The work suggested the possibility of measuring time variations of the spectral emissivity for metal surfaces in oxidation processes. The spectral emissivity may lead to more direct contribution than the spectral reflectivity to radiation thermometry.

This paper describes a system for measuring the spectral distribution of normal emissivity of metals in a wide wavelength range for a short period in various environmental conditions including oxidation. Attention was paid to increase the measurement efficiency in order to measure a large number of specimens for developing a normal spectral emissivity database consisting of a wide variety of metals.

2. MEASUREMENT SYSTEM

The measurement system consists of specimens, a multiband radiation thermometer for the specimen radiance measurement, a single-band radiation thermometer for the specimen temperature measurement, and a specimen heating/environmental control system.

Figure 1 shows a schematic of the measurement system. The front surface of the specimen heated by passing a direct current was observed at the middle of the specimen by the multiband radiation thermometer to measure the spectral radiance. The specimen temperature was measured from the rear by the single-band (0.9-μm) radiation thermometer. The normal spectral emissivity of the specimen was derived from the temperature measured by the single-band radiation thermometer and the spectral radiance on the specimen front surface at the normal direction measured by the multiband radiation thermometer.

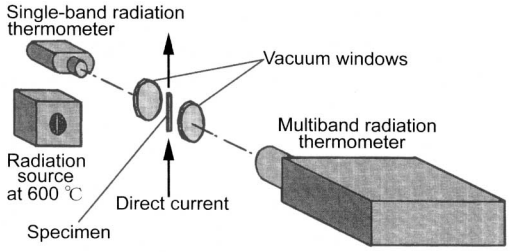

Fig. 1. Schematic of measurement system.

Surface oxidation of the specimen was controlled by introduction of oxidizing gases into a vacuum chamber. A change of atmospheric absorption due to water vapor and carbon dioxide along the optical path of the multiband radiation thermometer was corrected in such a way that a radiation source with a small black plate heated at 600° C was located in the atmosphere near the vacuum windows of the chambers, and it was observed by the multiband radiation thermometer periodically.

Figure 2 shows a standard shape of specimens and a specimen heating assembly. A sheet for a specimen 0.1 to 0.5 mm thick was folded in such a way that the specimen formed a cavity with an opening slit on the rear.

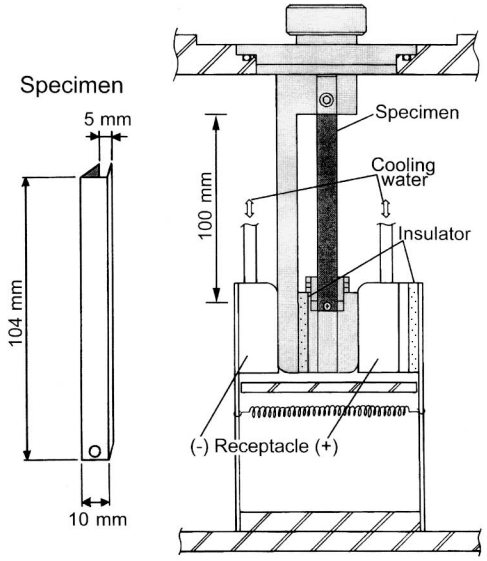

Fig. 2. Standard shape of specimen, specimen holder, and heating assembly.

The inner surface of the cavity was coated with heat-resisting black paint (Asahipen, Japan). The cavity was observed at the middle of the opening slit by the single-band radiation thermometer to measure the specimen temperature. Forming a cavity in the specimen as shown in Fig. 1 increases the effective emissivity and reduces the influence of degradation of the heat-resisting paint.

Figure 2 also shows a specimen holder and a receptacle cooled by water flow. The specimen holder has a flexible lead of bent copper ribbon that connects the bottom of the specimen and the lower electrode to absorb the thermal expansion of the specimen when heated. The specimen was tied to the specimen holder by two screws and a nickel bit to make good electric contact. The specimen holder was attached to one of the vacuum chambers and the receptacle using plug-type connections. Several specimen holders of such a plug-type were prepared to improve the measurement efficiency.

A total of thirty kinds of pure metals and alloys was prepared. Specimens were heated to high temperatures by passing a direct current. A power source of 500 A with a current regulator was used under manual control.

Figure 3 shows a front view of the specimen heating and environmental control system. It consists of two vacuum chambers of the same design; one is used for preheating of specimens and the other for emissivity measurements. Specimens are transferred from one chamber to another. The preheating is necessary to keep the vacuum window clean for measurements. The two vacuum chambers improved the measurement efficiency to accommodate a large number of specimens.

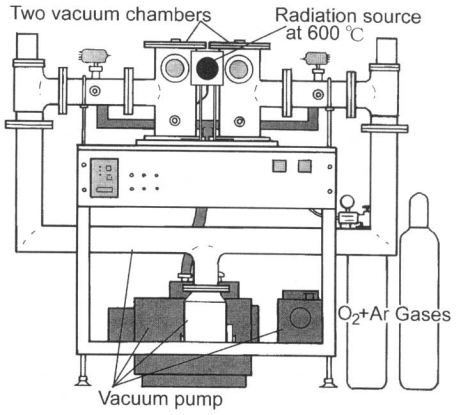

Fig. 3. Front view of specimen heating and environmental control system.

The chambers were evacuated by a turbomolecular pump. The air or argon gas with an oxygen density from 100 ppm to 10% was introduced into the vacuum chamber 7 L in volume for oxidation control of the specimen surface. The flow rate of oxidizing gas was regulated by a mass flow controller. The inner surfaces of the vacuum chambers were coated with the heat-resisting black paint to reduce reflection.

Figure 4 shows the optical system of the multiband radiation thermometer with 112 wavelengths. It consists of an objective optics with a pointing laser, a 64-element silicon/germanium hybrid linear array detector with a holographic grating ranging from 0.5 to 1.6 μm, and a 48-element InSb linear array detector with a LiF prism ranging from 1.3 to 5.3 μm. The use of linear array detectors eliminated mechanisms for grating and prism rotating. Reduction of background thermal radiation onto the InSb detector by using a large-size cold radiation shield contributed to stabilization of the zero level of the multiband radiation thermometer which eliminated a need for a mechanical chopper for incident radiation.

The readout electronics consists of 112 first-stage amplifiers, 7 FET multiplexers, 7 gain-adjuster amplifiers, a 12-bit A/D converter, and a personal computer. The optical system and the electric circuit realized a

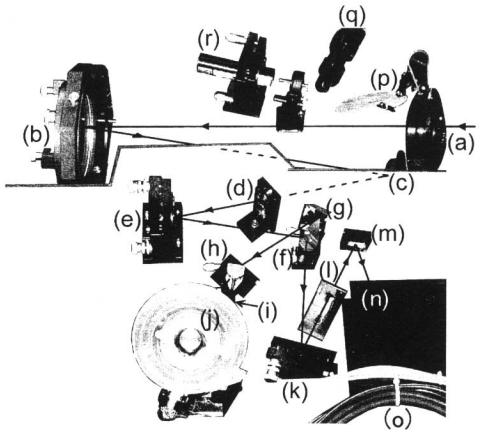

Fig. 4. Optical system of multiband radiation thermometer. (a) window, (b) objective mirror, (c) folding mirror, (d) aperture mirror, (e) collimator mirror, (f) beam splitter, (g) folding mirror, (h) LiF prism, (i) KBr lens, (j) InSb detector, (k) focusing mirror, (l) entrance slit, (m) grating, (n) silicon/germanium hybrid detector, (o) cooling liquid, (p) shutter, (q) finder, and (r) laser.

repetitive measurement time as short as 256 μs to scan a total of 112 wavelengths.

The multiband radiation thermometer was operated with a period of 0.5 or 1 s to reduce the amount of output data in actual measurements considering that the period was short enough to follow the emissivity and temperature changes. Ten A/D conversions for the integration and an automatic gain adjustment of the analog signal were made to each channel of 112 wavelengths every 0.5 s.

Before the normal spectral emissivity measurement, the single-band and multiband radiation thermometers were radiometrically calibrated against a standard radiation thermometer with the operating wavelength of 0.9 μm that had an accurate temperature scale established by fixed-point blackbody calibrations. In the radiometric calibrations a radiation source for atmospheric absorption correction and two variable-temperature blackbody furnaces were employed. The wavelength calibration of the multiband radiation thermometer was made by using 24 narrow-bandpass filters.

The surface roughness of the specimen front surface was measured at the middle of each specimen by a contact-type probe after cleaning the front surface with methanol. Then the specimen was tied to the specimen holder. Since the specimen had volatile matter and the heat-resisting paint required hardening, it was slowly preheated up to 600°C in one of the vacuum chambers. When the normal spectral emissivity was measured in a vacuum, the specimen was heated in the other vacuum chamber, and then the temperature was varied. When the normal spectral emissivity was measured in an oxidizing environment, the specimen was heated to a certain temperature in the vacuum chamber for measurements, and then a valve of the vacuum pump was closed and an oxidizing gas was introduced.

3. RESULTS AND DISCUSSION

3.1. Effective Emissivity of Specimen Cavity

The effective normal spectral emissivity of the specimen rear side was considerably increased by forming a cavity. However, it could not be regarded yet as a perfect blackbody. Hence, the specimen temperature was corrected for the effective emissivity.

The effective normal spectral emissivity of the specimen cavity was measured by comparison with that of a metal tube having a small hole at the middle. The metal tube was made by welding from a sheet of cold-rolled steel. All specimens used for the comparison were made from the same sheet as the metal tube. The front surfaces of the specimens and the

metal tube, and the inner surfaces of the specimen cavities and the metal tube, were coated with the same heat-resisting black paint.

The measurement was made as follows. First, a specimen was heated to a high temperature. Then the radiance temperature of the specimen cavity was measured, and the spectral radiance of the painted front surface was monitored by the multiband radiation thermometer at a wavelength of 2.13 μm, where the radiance resolution was sufficient. Second, the metal tube was heated to the same temperature as the specimen so that the monitoring multiband radiation thermometer indicated the same level of the spectral radiance of the painted front surface of the metal tube. The oxidizing environment and the temperature history were also set in the same way as the specimen. Third, the radiance temperature of the small hole was measured by the single-band radiation thermometer. The small difference between the radiance temperatures of the specimen and the metal tube was corrected.

The normal spectral emissivity of the specimen cavities was determined assuming that the effective emissivity of the small hole formed on the metal tube was unity and that the emissivity of the painted front surface of the metal tube was the same as that of the painted front surfaces of the specimens. Figure 5 shows the effective normal spectral emissivity of the specimen cavities in the course of measurement time that was determined at the middle of the specimen rear slit at the wavelength of 0.9 μm under

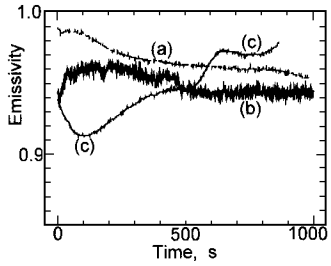

Fig. 5. Effective normal spectral emissivity of specimen cavities at the wavelength of 0.9 μm. The specimens were painted sheets of cold-rolled steel. (a) The specimen was heated at 1000°C in a vacuum; (b) the temperature was kept at 800°C and air was introduced into the vacuum chamber at a constant flow rate of 1 $cm^3 \cdot min^{-1}$; (c) the temperature was kept at 1000°C and air was introduced at a constant flow rate of 10 $cm^3 \cdot min^{-1}$.

three environmental conditions; see the figure caption. The effective normal spectral emissivity of the cavities ranged from 0.91 to 0.99.

The temperature dependence of the effective normal spectral emissivity was also measured in the range from 780 to 1100°C, and it could not be measured at temperatures above 1100°C because the cold-rolled steel specimens deformed and the paint came off the metal surfaces. The effective normal spectral emissivity ranged between a minimum value of 0.93 and a maximum of 0.97.

3.2. Uncertainty of Emissivity Measurements

Table I lists uncertainty estimates of the emissivity measurement. Uncertainties in the temperature scales include that in the standard radiation thermometer and that in the emissivities of the blackbody furnaces used for the calibration. In the short-wavelength range from 0.5 to 1.6 μm, the uncertainty of the effective emissivity of the specimen cavity was the largest except for low-temperature measurements and low-emissivity specimens. On the other hand, it was not dominant in the long wavelength range.

The total uncertainty was estimated to be 5%, or larger, of the emissivity value depending on the emissivity, temperature, and wavelength. The lower-temperature limit of the measurement and the total uncertainty at the short-wavelength range were determined from noise levels of the multiband radiation thermometer; the signal-to-noise ratio at a wavelength of 0.55 μm was 18 and that at 0.66 μm was 96 under the condition that the target was a blackbody furnace at 1052°C and the time constant of the electric circuit was 100 μs.

Table I. Uncertainty Estimates of the Emissivity Measurement System

	Uncertainty (% of the emissivity value)			
Wavelength (μm)	0.9	0.9	3.7	3.7
Emissivity	0.1	0.9	0.1	0.9
Souce of uncertainty				
Temperature scale				
Single-band thermometer	1	1	0.2	0.2
Multiband thermometer	1.5	1.5	2	2
Drift and noise of multiband thermometer	4	3	3	3
Effective emissivity of specimen cavity	5	5	1.5	1.5
Reflection at inner surfaces of vacuum chamber	5	0.5	5	0.5
Absorption of vacuum window and optical pass	2	2	3	3
Combined uncertainty	8.4	6.4	7.0	4.9

3.3. Examples of Emissivity Data

Figure 6 shows a time variation in the normal spectral emissivity of an Inconel 625 specimen in an oxidation process at 1000°C. A valve of the vacuum pump was closed at zero time, and then air was introduced into the vacuum chamber. The average surface roughness in the vertical direction was 0.12 μm. It is shown that the normal spectral emissivity changes in a systematic way as oxidation progresses. Oscillations of the emissivity appeared at the shorter wavelengths after the rapid rising of the emissivity, and then the peaks and the valleys in the oscillations shifted to the longer wavelengths. It can be concluded that the oscillations were caused by interference of emitted radiation in a growing oxide film on the specimen surface. The specimen color had changed from shiny to black after the measurement.

Figure 7 shows a time variation in the normal spectral emissivity of a Monel specimen that had been oxidized in the atmosphere of the room at about 1000°C before the emissivity measurement. In the emissivity measurement, the specimen temperature was increased from 773 (a) to 1157°C (b) and then decreased to 998°C (c) in a vacuum. The average surface roughness in the vertical direction was 0.43 μm. While the specimen color was gray before the measurement, it changed to shiny after that. The normal spectral emissivity at (c) is typical of clean surfaces of Monel specimens without oxidation.

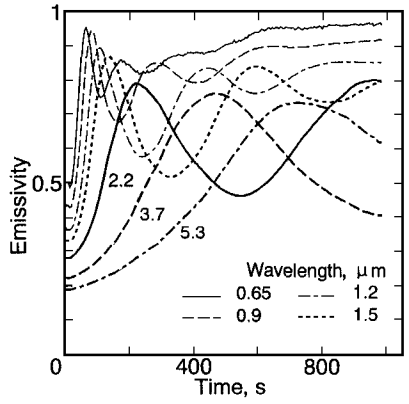

Fig. 6. Time variation in the normal spectral emissivity of an Inconel 625 specimen kept at 1000°C when air was introduced into the vacuum chamber at a constant flow rate of 1 $cm^3 \cdot min^{-1}$ (from 0 to 500 s) and then at 10 $cm^3 \cdot min^{-1}$ (from 500 to 1000 s).

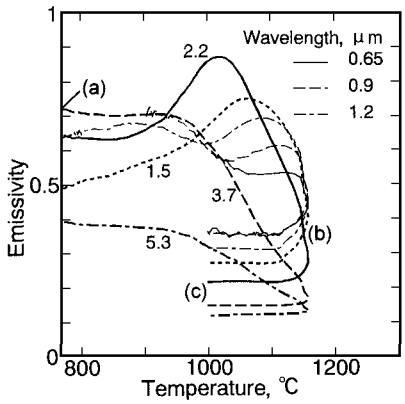

Fig. 7. Time variation in the normal spectral emissivity of a Monel specimen when varying the temperature in a vacuum. The specimen was oxidized by heating to about 1000°C in the atmosphere before the measurement. (a) The beginning of the measurement; (b) intermediate stage at the maximum temperature; (c) the end of the measurement.

4. CONCLUSIONS

Time variations in the normal spectral emissivity of metal surfaces in oxidation processes were observed by the emissivity measurement with a sufficiently small time interval. The data throughput of the measurement system was such that one measurement could be finished in an hour, including the setting time of the specimen.

REFERENCES

1. T. Makino, T. Kosaka, J. Arima, S. Aoyama, and H. Tsujimura, *Trans. SICE* **24**(4):331 (1988).
2. F. Tanaka and D. P. DeWitt, *Heat Transfer Measurement Analysis and Flow Visualization*, HTD-Vol. 112, 69 (1989).
3. K. Hiramoto, T. Yamamoto, and C. Uematsu, *Proc. 13th IMECO* (1994), p. 1456.
4. G. Ruffino, *Int. J. Thermophys.* **13**:165 (1992).
5. T. Makino, *Proc. 7th Jpn. Symp. Thermophys. Prop.* (1986), p. 37.
6. T. Makino, K. Kaga, and B. D. Brajuskovic, *Proc. 2nd Asian Thermophys. Prop. Conf.* (1989), p. 221.